Chapter 2

Forecasting Weather in Croatia Using ALADIN Numerical Weather Prediction Model

Martina Tudor, Stjepan Ivatek-Šahdan,
Antiono Stanešić, Kristian Horvath and Alica Bajić

Additional information is available at the end of the chapter

http://dx.doi.org/10.5772/55698

1. Introduction

Numerical weather prediction (NWP) models are one of the factors contributing to the complex process of providing an accurate weather forecast. A number of global NWP models forecast weather over the whole Earth seven or more days in advance. These large scale global models do not provide high-resolution details that can be important for the weather we feel in a particular point (sensible weather). These details are often provided by limited area models (LAMs) that cover a particular area of interest as will be exemplified in this chapter. The Croatian Meteorological and Hydrological Service (CMHS) uses ALADIN (Aire Limitée Adaptation Dynamique développement InterNational, ALADIN International Team, 1997) limited area model for the operational weather forecast. This chapter describes the operational NWP aspects in CMHS and provides an insight into high impact weather phenomena that are typical for this region.

The quality of NWP model forecast depends on the NWP model that is used to compute the meteorological forecast fields. Model forecast should improve with the improvements in the model equations and parameterizations used to describe the atmospheric processes (Pielke 2002, Durran 1999, Werner et. al 1997). Another factor is the quality and availability of the measured atmospheric data used as input for the data assimilation procedure that creates the initial conditions for the model forecast. Limited area models also require the lateral boundary conditions data which are another factor contributing to the quality of the weather forecast. Both initial and lateral boundary conditions are usually taken from a larger scale and lower resolution NWP model covering larger geographical area. The initial conditions can be modified using a local initialization procedure.

The operational forecast suite in CMHS uses the initial lateral boundary conditions from the ARPEGE (Action de Recherche Petite Echelle Grande Echelle, http://www.cnrm.meteo.fr/gmapdoc/meshtml/guide_ARP/arpege.html) global NWP model run operationally at Meteo-France. Another set of initial and boundary conditions available in CMHS is from the Integrated Forecast System (IFS, http://www.ecmwf.int/research/ifsdocs/CY36r1/ index.html) of the European Centre for Medium-Range Weather Forecast (ECMWF).

The files received from Meteo-France and ECMWF do not contain the global model fields covering the whole Earth on the native ARPEGE or IFS grid and model levels. To optimize the data transfer, the model data is interpolated to a limited-area Lambert projection grid in a resolution similar to the one of the global model in that area and it is covering a wider geographical area than the local LAM that uses it. Since ALADIN is a spectral model, initial and boundary conditions contain the meteorological data covering the whole model domain in the form of spectral coefficients, and not only the data on the lateral boundaries.

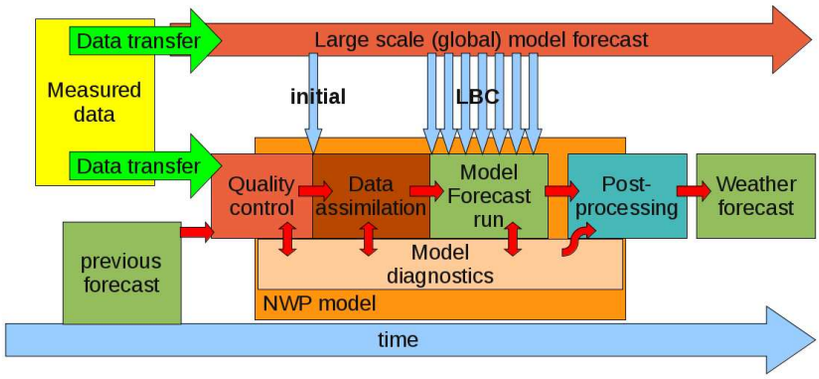

Figure 1. The scheme of the steps taken when making the weather forecast

The number of levels in the vertical is reduced (from 70 in ARPEGE or 91 in IFS to 37 in ALADIN Croatia), since LAM does not have to reach as high in the atmosphere as the global models. The global models have considerably longer forecast range (10 to 15 days in advance) that require knowledge of the atmospheric processes as high as the stratosphere top and mesosphere. These processes have negligible impact in the 72 hour forecast range used for the operational ALADIN forecast in CMHS..

The forecast process (Fig 1) consists of several steps:

1. collect the measured data representative for the initial forecast time from upper-air soundings, surface stations, meteorological satellites, aircraft and radar data,
2. data quality control which removes measurements if values are too far from the first guess, removal of observations according to empirical (black)list and surface observations with too large height difference between model orography and real station height.
3. establishment of the initial and lateral boundary conditions using data obtained from a larger scale (global) model,

http://dx.doi.org/10.5772/55698

4. the NWP model forecast run that consists of:

a. the data assimilation procedure that produces the analysis ("best possible" approximation of atmospheric initial conditions for the model forecast run),

b. the NWP model forecast,

c. diagnostics of the derived parameters from the model variables during the forecast run,

5. post-processing of the model output data.

Weather forecasts are time-critical applications. This means that the value of the products quickly degrades with time. In other words, the model forecast run has to finish before a certain time in the day, according to the requirements of the users. The choices of the input data and the model complexity that are used operationally also depend on the hour at which the weather forecast products should be available to the users. It is desired to keep the time span between the data measurements and the availability of the weather forecast as short as possible or within a reasonable interval usually determined by procedures in the forecast office or requirements of the other users. The time required for each forecast step in Figure 1 is determined by technical limitations such as the capacity of data transfer to the institution providing the weather forecast as well as the speed of the mainframe computer executing the NWP model software. The amount of data used in points (1) and (2) is limited by the capacity of data storages and speed of the data transfer lines. The complexity of the operational NWP model, as well as the size and grid resolution of the model domain is determined by this time span and the computer power. ARPEGE model data was the primary choice for the ALADIN operational model input in CMHS since it is available much earlier than the IFS model data (Fig 2). IFS is available later than ARPEGE because the data assimilation procedure starts later since it waits to assimilate more measured data. On the other hand, ARPEGE provides two sets of input data, as will be described later.

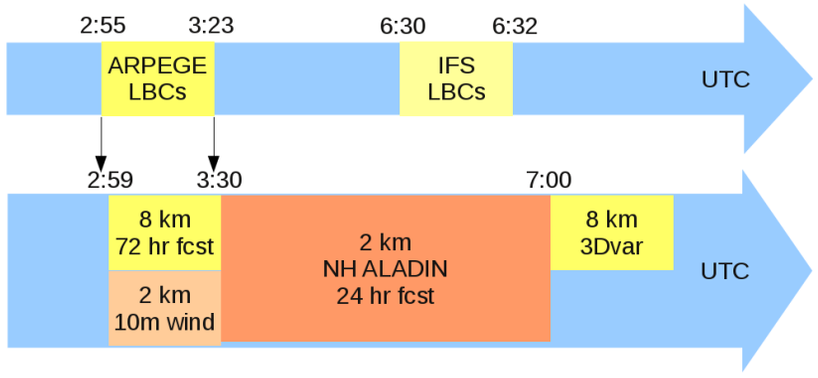

Figure 2. The schedule and timing of the 00 UTC operational run in August 2011.

A considerable effort in the research and development of the ALADIN model has been devoted to the model optimization and various model options with an aim to provide the best possible forecast in the short time using available computer power (Yessad, 2011). To improve the 10

m wind forecast in severe wind situations, like bura (local name for bora) windstorms, a procedure that provides a high resolution forecast of the wind 10 m above ground has been established. The high-resolution dynamical adaptation (HRDA) of the wind field using a hydrostatic version of the ALADIN model has been introduced to the operational suite soon after the 8 km resolution operational forecast runs have started in 2000 (Ivatek-Šahdan & Tudor, 2004).

2. Operational model characteristics

ALADIN has been developed by a group of scientists from 16 countries and shares a considerable part with the global models IFS and ARPEGE. Both global models are a result of a coordinated effort of ECMWF and Meteo-France. Another LAM developed on the basis of IFS global model is HIRLAM (High Resolution Limited Area Model, Unden et al 2002). These models share the same source code in many parts of the model. A considerable part of the dynamics and data assimilation is in common too. ALADIN can use the same vertical discretization, grid-point dynamics and the various physics options as the global model ARPEGE. This section describes the operational model characteristics, the domains and other options used in the operational suite.

2.1. Model domains used in the operational suite

The operational ALADIN model forecast is run on a Lambert-projection domain with 8 km horizontal resolution (Fig 3). The model fields are subsequently going through a dynamical adaptation procedure (Ivatek-Šahdan & Tudor, 2004) that produces 2 km resolution forecast of 10 m wind speed and gusts for a smaller domain shown in Figure 3. The procedure adapts the wind field of the 8 km resolution forecast and uses hydrostatic set-up of the ALADIN model with turbulence parameterization only. As an addition to the operational forecast, a 2 km resolution 24 hour forecast was established recently, that uses non-hydrostatic (NH) dynamics and the full parameterization set, including radiation, microphysics and convection schemes. This forecast is run for the same small domain (Fig 3).

2.2. Initialization and data assimilation

In the ALADIN community, the initial conditions for the model forecast can be obtained using different approaches:

1. using the large scale model data as initial conditions,
2. blending the large scale information from low resolution global model fields with the high resolution features from the previous LAM forecast,
3. using the data-assimilation procedure.

The first approach is used operationally in CMHS since the beginnings of the operational ALADIN forecast suite in 2000. There the upper-air and surface fields are taken from the

http://dx.doi.org/10.5772/55698

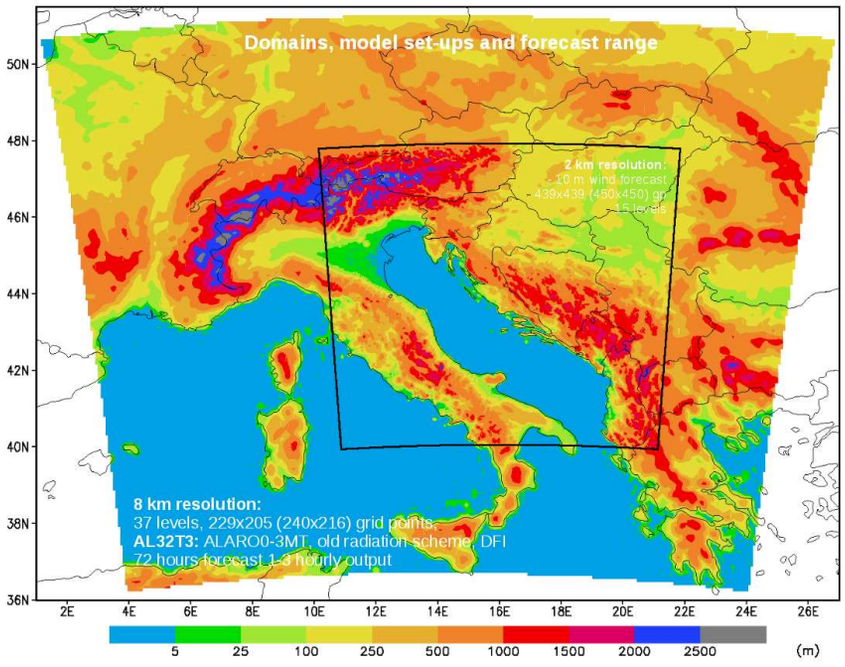

Figure 3. The ALADIN model domains and terrain height used operationally in CMHS.

ARPEGE global model and interpolated to the ALADIN grid. Afterwards, these fields are balanced using digital filter initialization (DFI) procedure (Lynch & Huang, 1994). However, the removal of the high-frequency wave energy from the initial conditions also affects the fast meteorological waves. Termonia (2008) showed how DFI can significantly reduce the depth of the eye of the storm and proposes a solution in the scale-selective DFI (SSDFI).

The second approach has not been used in CMHS, but blending has been used extensively in the ALADIN operational forecast suite in the Czech Meteorological and Hydrological Institute (CHMI, Brožkova et. al., 2001) as well as several other ALADIN member services (Hdidou, 2006). The blending procedure makes use of the fact that ALADIN is a spectral model. The initial model fields are constructed from the long waves coming from the low resolution model (ARPEGE) and short waves from the high resolution model (ALADIN).

The last approach is to initialize ALADIN model using data assimilation and currently it is used in experimental configuration in CMHS. Data assimilation is a procedure wherein information coming from measurements is combined with some a priori estimate (usually a short range forecast often called first-guess or background field) and their associated observation and background model errors, respecting the model dynamical balances, to get the analysis - a maximal likelihood or "as best as possible" approximation of the true state of the atmosphere at a given time. There are different methods of solving this analysis problem (Hólm 2008) and at CMHS two of them are used: the optimal interpolation (OI, Courtier 1999) and the variational method (3DVAR, Hollingsworth et al, 1998). Optimal interpolation is used for updating land surface fields while 3DVAR is used for analysis of upper air fields. It was shown by Mahfouf (1991) that 2m analysis increments of temperature and humidity computed with OI can be used to update the land surface variables. As only the increments of 2m temperature

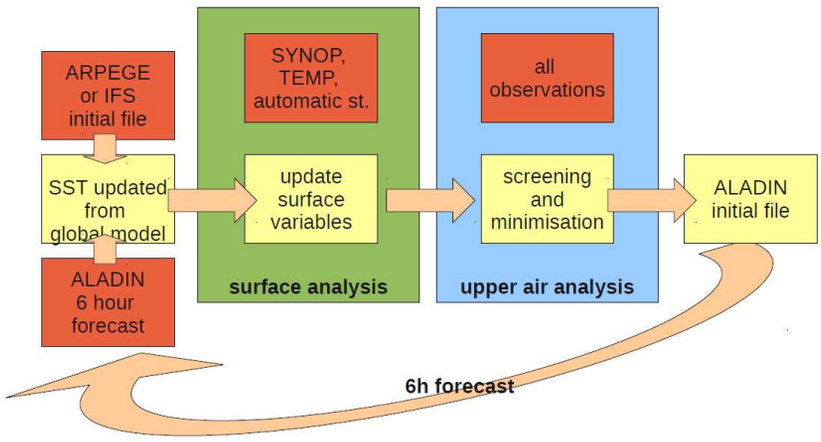

Figure 4. Schematic view of the data assimilation cycle.

and relative humidity are needed, and only the surface measurements are used, rather simple OI method was implemented for computing the 2m analysis increments. For the upper air fields more control variables are defined, more sources of data are used, and more sophisticated variational algorithm (3DVAR) is implemented. 3DVAR belongs to the group of intermittent variational data assimilation strategies, and whereas the true state of the atmosphere is never known, the principal challenge in determining the analysis is to estimate the background (model) errors. Namely, knowledge of the background error statistics is used to derive the analysis increments and transfer this information in horizontal and vertical directions in the atmosphere. The background error statistics is in CMHS estimated by using the so-called standard NMC method. In this approach, background error statistics is derived from a set of differences between forecasts that are valid at the same time, but at different forecast horizons, typically 12 and 36 hours. In addition, the multivariate formulation of the background error statistics that uses vorticity, divergence, temperature and surface pressure, and humidity as control variables (Berre, 2000), allows the propagation of the analysis increments from one to all the other variables, and thus increases the effect of each single observation. Finally, the potential use of the ensemble and seasonal formulations of the background error statistics is currently being investigated.

Practical implementation of data assimilation setup in CMHS is illustrated in Figure 4 that shows the scheme of one assimilation cycle. Because of limited computer resources the assimilation cycle is run in quasi-operational mode i.e. observation data is taken at the operational time, but the assimilation procedure is performed with certain time delay. An assimilation cycle is a sequence of a 6 hour forecast and analysis that is run on a daily basis. In the first step, SST in the 6h forecast from previous cycle (background) is replaced with SST taken from global model ARPEGE analysis. This replacement is done because no local SST analysis is implemented. In the second step, the background land surface variables are updated. As there are almost no or very little surface observations available, 2m observations are used to retrieve information about the surface temperature and soil water content. Therefore, after the quality control of the 2m observations, an optimal interpolation is used to

http://dx.doi.org/10.5772/55698

calculate increments of 2m temperature and relative humidity. These increments in a more or less sophisticated way are propagated into the land surface equivalents and used for updating the land surface variables. In the next step, the background upper air fields are analysed using 3DVAR. The standard NMC background error statistics is calculated by the aforementioned procedure over a 100-day period, from 15 Feb – 25 May 2008. The background error matrix was not tuned a posteriori such as in some other NWP systems (Bölöni and Horvath, 2010). The 3DVAR procedure includes a quality control of available data (screening) and minimization procedure that as output produces an analysis which is used for initiating the 6h forecast. The assimilation cycle is repeated every 6 hours, at 00, 06, 12 and 18 UTC. It is also run with a time delay big enough to enable usage of long cut off ARPEGE coupling files (the ARPEGE model is run later and in assimilation all data is used) for boundary conditions of 6h ALADIN forecast. Also long cut off data is used in cycle (data available after the time period needed to collect all observations of interest). Production from the assimilation cycle is done following same steps as in the assimilation cycle but at its end, a 72h forecast is performed. However, to perform a quasi-operational 72 hours forecast, timing constrain does not allow to use long cut off data and long cut off ARPEGE files; thus short cut off data and ARPEGE files are used.

2.3. Model dynamics

The NWP model characteristics are usually described in the terms of the model numerics, dynamics and physics. Model numerics refers to the model computational domain, coordinate system, model resolution and grid as well as the mathematical methods used to solve the system of the prognostic differential equations.

Model dynamics refers to the resolvable processes that are resolved by the model grid and described by the set of model equations for horizontal and vertical momentum and conservation of mass and thermodynamic properties. These processes encompass advection, pressure gradient force and adiabatic changes of heat/temperature.

The model dynamics is computed using semi-implicit time integration scheme (Robert, 1982). An implicit treatment of the gravity wave equation is absolutely stable (Durran, 1999). The semi-implicit scheme treats implicitly only a linearized form of the adjustment terms in the shallow water equations. The method results in solving the Helmholtz equation in spectral space.

ALADIN is a shallow-water spectral limited-area model. It applies Fourier spectral representation of the model variables. That allows the advantage of fast Fourier transforms (FFTs) in both directions. An elliptic truncation that limits the Fourier series (Machenhauer & Haugen, 1987) ensures an isotropic horizontal resolution. The number of grid points in each horizontal direction of the whole integration area (N) is chosen so that $N>3M+1$, where M is the truncation wave-number in the same direction. This representation ensures that the nonlinear terms of the model equations are computed without aliasing. The model fields are transferred from spectral to grid-point space and back in each model time step.

The accumulation of energy at the shortest wavelengths, due to spectral blocking, is reduced by a common 4th order numerical diffusion at the end of the time step. Semi-Lagrangian

interpolators can be more or less diffusive (Staniforth and Cote, 1991). Combining two interpolators of different diffusivity with the flow deformation as a weighting factor yields more physical horizontal diffusion scheme that is based on the physical properties of the flow (Vana et al., 2008). This semi-Lagrangian horizontal diffusion (SLHD) is combined with numerical diffusion that removes short waves from the high layers of the atmosphere.

The advection of the prognostic variables in the model is computed using two-time-level semi-Lagrangian scheme. The method takes the model grid-points as the arrival points of the trajectory. The trajectories are computed one time step backwards to the origin points.

The model prognostic variables that are involved in the semi-implicit computations in the hydrostatic version of the model are surface pressure, the horizontal wind components, temperature and water vapour. The non-hydrostatic dynamics involves two additional model variables: pressure departure and vertical divergence that are treated by the semi-implicit computations. The developments in physics have introduced more prognostic variables to the model, such as cloud water and ice, rain and snow, as well as convective updraft and down-draft vertical velocities and mesh fractions. These quantities can be (optionally) advected by the semi-Lagrangian scheme and diffused by SLHD but do not enter the semi-implicit computations. In the operational forecast run, all these variables are advected, but SLHD is applied only to water vapour, cloud water and ice. This configuration supports modelling the advection in the atmospheric front, but may spoil the forecast of rainfall due to orography or other local feature that does not move with the flow,

The finite difference method is used to solve the model equations in the vertical, on 37 levels of hybrid pressure type eta coordinate (Simmons & Burridge, 1981). The primitive prognostic equations are solved for the prognostic variables using the two time level, semi-implicit, semi-Lagrangian advection scheme with a second-order accurate treatment of the nonlinear residual (Gospodinov et al. 2001).

2.4. Lateral boundary conditions and coupling

LAM uses the large scale model data in a narrow coupling zone on the lateral boundaries and at discrete time intervals. The coupling of the model variables is done using Davies (1976) relaxation scheme in a narrow zone on the lateral boundaries of the LAM domain (Fig 5). The model dynamics requires usage of time dependent and periodic LBCs (Haugen & Machenhauer, 1993). The coupling procedure has to be applied at the very beginning or end of the grid-point computations (Radnoti, 1995) due to constraints imposed by the model dynamics. Various schemes for the lateral boundary treatment are associated to different problems (Davies, 1983). Werner et al. (1997) give an overview of weaknesses of the LAM forecast caused by the LBCs.

The lateral boundary conditions (LBC) are operationally obtained with a 3 hour interval. This interval is a compromise between the need to reduce the amount of data that have to be transferred and stored and the need to capture fast cyclones, fronts and other meteorological phenomena that can enter the LAM domain through its lateral boundaries. The coupling scheme requires large scale data in the coupling zone for each LAM time step. The large scale

http://dx.doi.org/10.5772/55698

model data in the coupling zone is interpolated linearly in time. The time span between the available LBC data of 3 hours and the coupling zone width is 8 grid-points in 8 km resolution. Three hours can be sufficiently long and 64 km can be narrow so that a particular meteorological feature can cross the coupling zone within the coupling interval (Fig 5). Solutions to this problem have been proposed, that include an alternative coupling scheme or interpolation in time (Tudor & Termonia, 2010), but have not been implemented to the operational model so far. The operational 2km resolution forecast uses LBC data from the operational 8 km resolution forecast with a 1 h interval.

In the two-way coupling approach, the flow information about the state of the atmosphere goes from the small-scale model to the large scale one, as well as in the opposite direction. This method requires simultaneous integration of both high and low resolution runs. For that reason, the operational 8km and 2 km resolution runs use one-way coupling that allows transfer of information only from the large-scale to the small-scale model run. The high resolution forecast starts only after the low resolution one is finished.

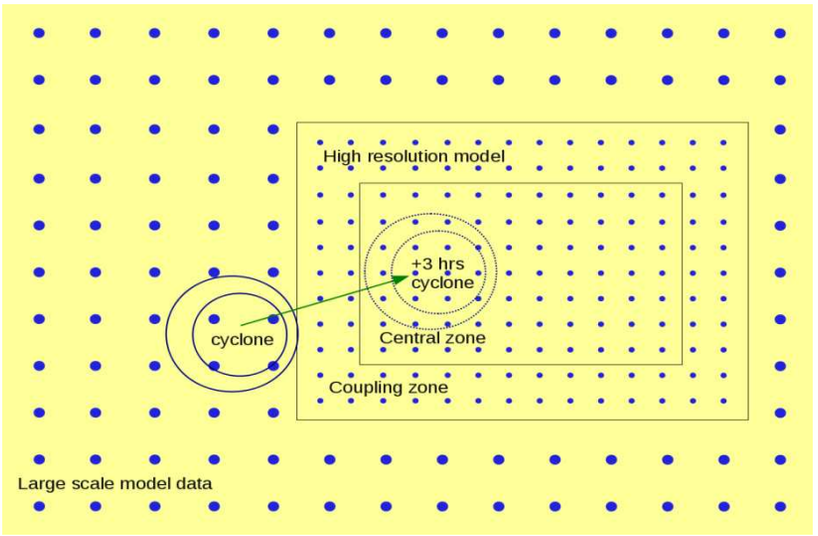

Figure 5. Schematic view illustrating the coupling problem.

2.5. Model physics

Model physics describe the processes unresolved by the model grid, radiation, cloud microphysics and surface processes. The processes described by the model physics are said to be parameterized (Pielke, 2002). The sub-grid-scale and diabatic processes are parameterized so their contribution to the changes in the large-scale state of the atmosphere can be considered.

The convective processes redistribute momentum, heat and moisture in the vertical. The deep convection parameterization (Fig 6) used in ALADIN (Gerard & Geleyn, 2005) is a prognostic mass-flux scheme (Gerard, 2007) where convective processes are treated with the use of prognostic variables for updraft and downdraft vertical velocities and mesh fractions (Gerard et al., 2009).

Cloud microphysics describe the processes of condensation, evaporation, freezing and melting as well as the processes that transform the cloud water droplets and ice crystals into rain and snow (Fig 6). ALADIN uses a simple microphysics scheme with prognostic cloud water and ice, rain and snow (Catry et al., 2007) and a statistical approach for sedimentation of precipitation (Geleyn et al., 2008). The microphysics scheme of the resolved processes is kept as close as possible to the original scheme that was without the prognostic condensates. The original scheme is the Kessler (1969) type scheme with modifications (Geleyn et. al. 1994) that include melting and freezing and imposing a brutal transition from ice to water at the temperature triple point.

The radiation processes described in the model encompass the transfer, scattering, absorption and reflection of the shortwave solar radiation and long-wave thermal radiation of the Earth's surface and clouds. There are several radiation schemes available in the ALADIN model (Morcrette, 1989, Mlawer et. al. 1997), but the simplest one is used in the operational version. The operational scheme (Ritter and Geleyn 1992) is based on Geleyn and Hollingsworth (1979) scheme. It is simple and computationally cheap since it uses only one spectral band for long-wave and one for short-wave radiation computations. The scheme has been enhanced recently (Geleyn et. al. 2005a, 2005b) but these modifications did not improve the cloud and temperature forecast in the stratus and fog case (Tudor, 2010).

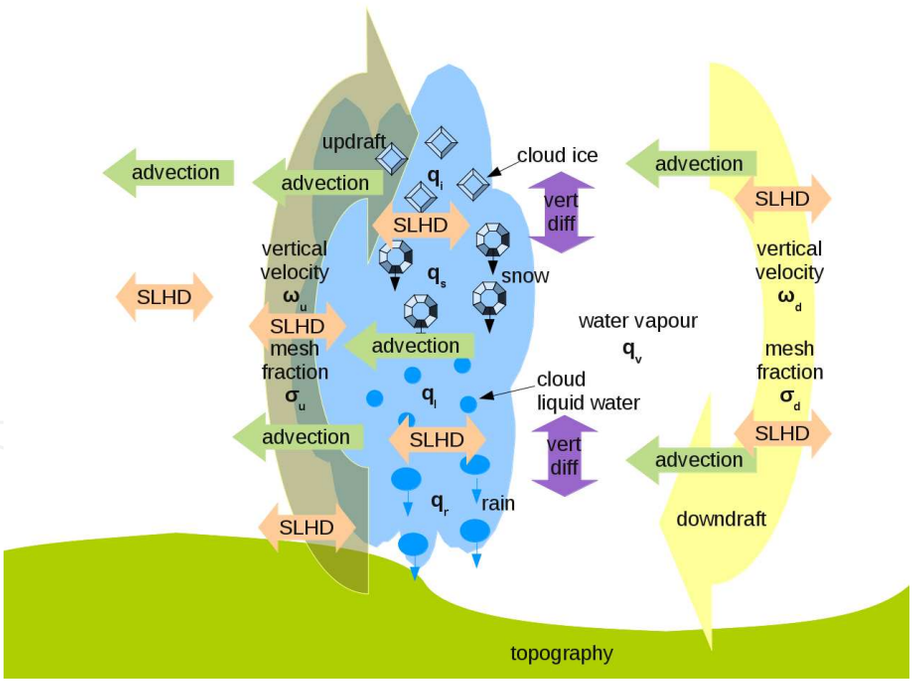

Figure 6. Schematic view of the scheme of the prognostic variables describing microphysics and convection and associated processes in the version of the ALADIN model used in CMHS.

The turbulence parametrization scheme describes the impact of the unresolved motion and surface roughness on the vertical transfer of heat, momentum and moisture. The turbulent exchange coefficients are modified from Louis et al. (1982) and are computed using prognos-

http://dx.doi.org/10.5772/55698

tic values of TKE (turbulent kinetic energy) according to Geleyn et al. (2006) and Redelsperger et al. (2001).

The gravity wave drag and lift parameterization scheme describes the vertical momentum flux due to the atmospheric waves generated by the unresolved topographic features. The surface parameterization schemes describe the soil properties and their impact on the meteorological model variables. ISBA (Interaction Soil Biosphere Atmosphere) is the surface scheme used in the operational forecast (Noilhan & Planton, 1989) as well as in the surface data assimilation (Giard & Bazile, 2000). The scheme describes the exchange of heat and moisture between land surface and air using thermal and hydrological properties of particular soil types (described with dominant land-use type, percentages of clay, sand and silt, useful soil depth, thermal roughness length) and vegetation changes during the year (described by vegetation fraction, leaf-area index, surface resistance to evapotranspiration). The prognostic variables are temperature, liquid and solid water contents are computed on two layers representing the soil surface and deep soil properties, and additional variables describe surface snow reservoir, density and albedo and ice and water on leaves. Snow budget depends on snow precipitation, evaporation and melting as well as snow accumulated on vegetation.

Each parameterization scheme obtains the information on the state of the atmosphere from the model variables and possibly output from other parameterizations. Then it uses a set of closure assumptions that relate the parameterized process to the state of the atmosphere. The parameterization schemes have the largest impact on the prediction of the sensible weather at the Earth's surface (Pielke, 2002). These schemes became more complex over time and interact with each other, the numerical and dynamical parts of the model.

Model diagnostics produces the numerical values of the sensible weather fields from the model variables, such as the accumulated precipitation, instantaneous cloudiness or maximum wind gusts. Wind, temperature and humidity are interpolated from the model levels to the standard meteorological measurement heights (10 and 2 meters above surface) using a parameterized profile (Geleyn, 1988).

2.6. High resolution dynamical adaptation

The Croatian mountains are relatively small in extend, many of them have width close to 10 km and length less than 50 km. But the mountain peaks reach over 1 km inland, and several mountain tops reach over 1.5 km very close to the coastline (Fig 3). These mountains are separated by deep and inhabited valleys while important roads and connections go through the mountain passes.

Weather in Croatia is in many ways modified or even controlled by orography (Zaninović et. al. 2008), but the large scale models do not resolve many of these local weather patterns. These weather patterns result from interaction of synoptic forcing with orography. Improved representation of orography in a meteorological model is expected to improve the forecast of weather phenomena that are strongly influenced by local orography (Horvath et. al., 2011, Bajić, 2007, Branković et. al., 2008).

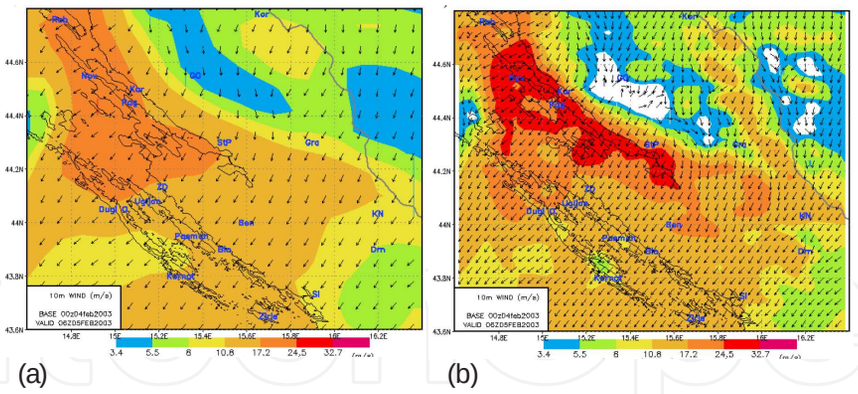

Figure 7. m wind forecast with 8 km (a) and 2 km resolution (b) for 6 UTC 5th Feb 2003.

The dynamical adaptation method of Žagar & Rakovec (1999) has been adapted for the purpose of operational forecast of the 10 m wind. The method provided successful operational forecast of the 10 m wind (Ivatek-Šahdan & Tudor, 2004) an has been used extensively in research impact studies (Bajić et al., 2007) as well as case studies (Tudor & Ivatek-Šahdan, 2002) of severe wind.

The meteorological model fields are first interpolated from the low resolution (8km in this case) to a higher resolution (2km) grid, but on considerably lower number of model levels, from 37 to 15 levels in the vertical. The number of vertical levels is reduced to minimize the computational cost. The levels close to the ground are of similar density, but the levels higher in the atmosphere are mostly omitted. Then a hydrostatic version of the ALADIN model is run for 30 time steps with a 60 second time step. The same large scale model data is used for the initial and LBC data, therefore the fields on the lateral boundaries do not change during the adaptation procedure. Turbulence is the only parameterization scheme used. Contributions from the moist and radiation processes are not computed to accelerate the model run.

HRDA improves 10 m wind forecast (by 15%), especially in weather situation with strong bura wind, since wind-speed and direction depend on the terrain configuration upstream. Figures 7a and 7b illustrates the impact of high resolution orography on the 10m wind forecast. HRDA wind is much weaker (reduces from 10-15 m/s to less than 5m/s) and changes the direction (up to 180°, depending on location) from the low resolution forecast in the valley upstream of the mountain. Downstream of the mountain, wind is much stronger (increases from 15 m/s in low resolution model to more than 30 m/s) in the high resolution model run as mountain wave breaks and windstorm reaches the mountain slope (Fig 8).

The 10 m wind forecast from HRDA has been used in several applications, and improved the safety of the traffic in the air, on the sea as well as on land. Unfortunately, there were also events of short bura episodes connected to a local pressure disturbance (Tudor & Ivatek-Šahdan, 2010) that were not predicted by HRDA. These were used in a further study to assess the impact of the neglected effects to these bura episodes. This procedure is able to forecast bura onset, duration and strength if it is a consequence of a synoptic forcing. It misses those cases initiated by small scale disturbances in the pressure fields. These disturbances have to be modelled first, using the non-hydrostatic model version on more levels in the vertical with

http://dx.doi.org/10.5772/55698

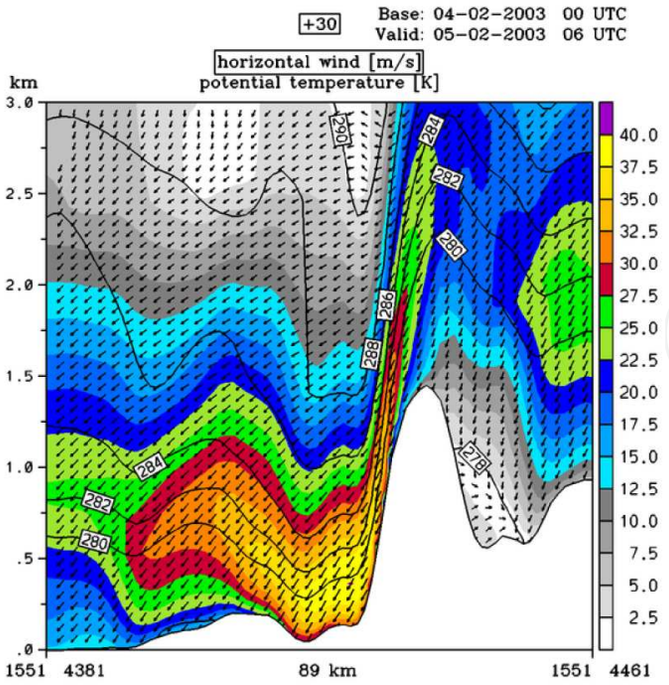

Figure 8. Vertical cross-section of wind speed (shaded), direction (vectors) and potential temperature (black isolines) for 6 UTC 5th Feb 2003.

full complexity of the physical parameterization package. These conclusions were based on analysis of a number cases of bura associated with a small scale pressure disturbance. Once a pressure disturbance is modelled, the wind field acts according to the measurements. The disturbances have to be detected first in the pressure measurements from the automatic stations that are performed on a less dense network than the wind measurements. The operational forecast using the latter configuration has been established only recently. The number of cases is still too short to make a thorough statistical analysis.

2.7. The operational forecast schedule

In CMHS, the operational ALADIN forecast is run twice per day, starting from 00 and 12 UTC analyses. The operational ALADIN model forecast is run 72 hours in advance on a Lambert-projection domain with 8 km horizontal resolution on 37 hybrid sigma-pressure levels in the vertical. The model fields are subsequently going through a dynamical adaptation procedure (Ivatek-Šahdan and Tudor, 2004) that produces 2 km resolution forecast of 10 m wind speed and gusts. There are two more sets of initial and LBC data available from both ARPEGE and IFS. The analyses at 06 and 18 UTC are used for cycling of the data-assimilation procedure. Only 6 hour forecasts are produced from these analyses and they are used as a first guess in the data assimilation procedure for the next analysis time (12 and 00 UTC) that initiates the 72 hour forecast. Alternative 8 km resolution 72 h forecasts run from the initial fields created in 00 and 12 UTC data-assimilation. These runs provide an alternative forecast fields that differs slightly from the first operational run. As an addition to the operational forecast, 2 km resolution 24 hour forecast was established recently, that uses the non-hydrostatic (NH)

dynamics in the ALADIN model and the ALADIN's full parameterization set, including the convection scheme. This forecast runs is performed once per day, following the 00 UTC operational 8 km resolution forecast. It uses the 6 hour forecast from the 8 km resolution operational run as input initial file and runs with SSDFI. This high-resolution forecast is run for 24 hours, until 6 UTC on the next day. This procedure allows covering the 24 hour period used to collect precipitation data from the rain-gauges.

2.8. Predictability

High impact weather events are often forecasted by means of their predictability. ALADIN has been used in several predictability studies (e.g. Branković et al., 2007) as well as the Limited Area Ensemble Forecasting (Wang et al., 2011) system. In most of these studies, ECMWF ensemble forecasts were dynamically downscaled for several severe weather cases. Therefore, the initial conditions come from perturbations generated by singular vectors of ECMWF. Wang et al. (2011) combined different initial and boundary conditions from the perturbed global model with other aspects of forecast uncertainty, such as blending, multi-physics approach and breeding.

Predictability studies of bura cases have found little sensitivity to different initial conditions (Ivatek-Šahdan & Ivančan-Picek, 2006). Horvath et al. (2009) suggested a small effect of uncertainties in the upstream initial conditions on the bura events in the southern Adriatic Sea. Another study of severe bura (Branković et al., 2007) exemplified a case of gale force bura that was predicted with a probability exceeding 95%. Dynamical downscaling of ECMWF fields from 40 to 8 km resolution improves the precipitation rate and pattern in the intensive precipitation cases (Branković et al., 2008) too, the predicted precipitation is roughly double in the high resolution forecasts, but still reaches only 20% of the observed precipitation maximum.

3. High impact weather events

The capability of the ALADIN model to predict high-impact weather events in Croatia is illustrated by several exemplary cases that encompass various weather types.

3.1. Bura (bora)

Bura is a local word describing a downslope windstorm on the eastern Adriatic coast. It is a northeasterly wind with high gustiness that is mostly controlled by the upstream topography of Dinaric Alps. During a windstorm episode, several roads and ferry lines to the islands get closed. The strength and variability of bura wind varies from case to case (e.g. Horvath et al., 2009) and reaches up to 69 m/s and varies in space, although several places became famous for it. The processes that control bura occurrence and strength are briefly illustrated. Grisogono & Belušić (2009) give a comprehensive review of recent advances in bura research.

http://dx.doi.org/10.5772/55698

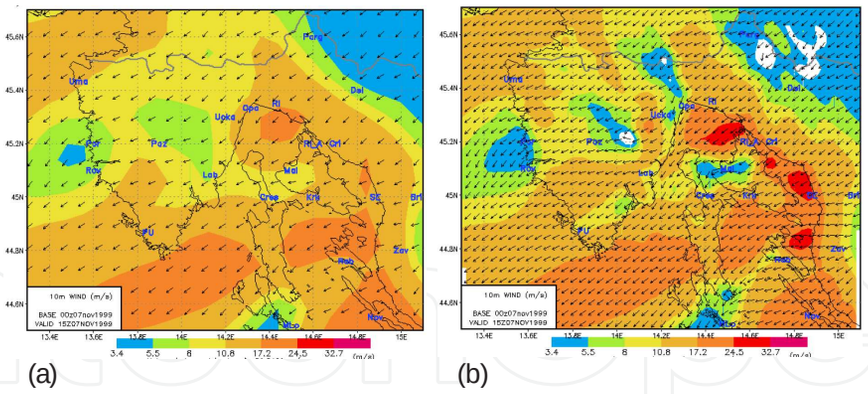

Figure 9. m wind forecast with 8 km (a) and 2 km resolution (b), for 15 UTC 7th Nov 1999.

MAP Special Observing Period 15 (SOP 15), from 7th to 9th Nov 1999, was characterized by severe bura on the eastern Adriatic Sea (Fig 9). The bura was associated with an intensive cyclone that was slowly moving over central Italy. A cold air outbreak from northeast intensified the pressure gradient over the coastal mountains and intensified wind in the lower layers of the atmosphere. During SOP 15, special measurements were taken from ELECTRA aircraft, through a northwest-southeast transect, parallel to the eastern Adriatic coast (Grubišić, 2004). The measurements were taken on levels 330 m and 660 m above the sea level and in the period from 15 to 16 UTC on 7th Nov 1999 (Fig 10). The 8km resolution forecast underestimated wind speed in the vicinity of the coastal mountains by 30% on average (Fig 9a). The wind forecast improved considerably (up to 10% over or under estimation of wind speed) using HRDA (Fig 9b). But the wind above the open sea (where the aircraft flew) was similar, both at surface (Fig 9) and at flight levels (Fig 10). The wind maximum at 660 m level is well predicted, as well as the northern minimum. The southern minimum is weaker by 5 m/s than measured and moved further south. On the lower level, at 330 m, model overestimates the maximum of the wind component normal to the flight direction by 3 m/s.

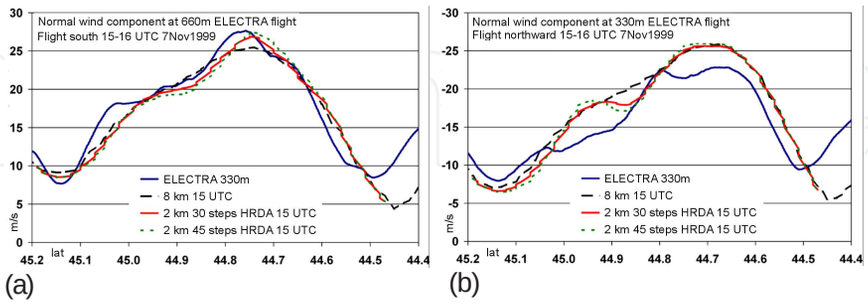

Figure 10. Comparison of measured and model normal wind components on flight levels 660 m (a) and 330 m, for 15-16 UTC 7th Nov 1999.

The strongest wind gust ever measured in Croatia was 69.0 m/s on Maslenica station (Bajić 2003) that was still operational during December 2003. During severe bura in that area, the 10 m wind speed is usually underestimated by the 8 km resolution forecast by 30 m/s on average

(Fig 11a). The HRDA forecast improves the surface wind forecast as it puts the wind speed maximum closer to the surface (Fig 11b), especially to the slope of the mountain as the mountain wave breaks. The wind maximum is still underestimated by 10-12%.

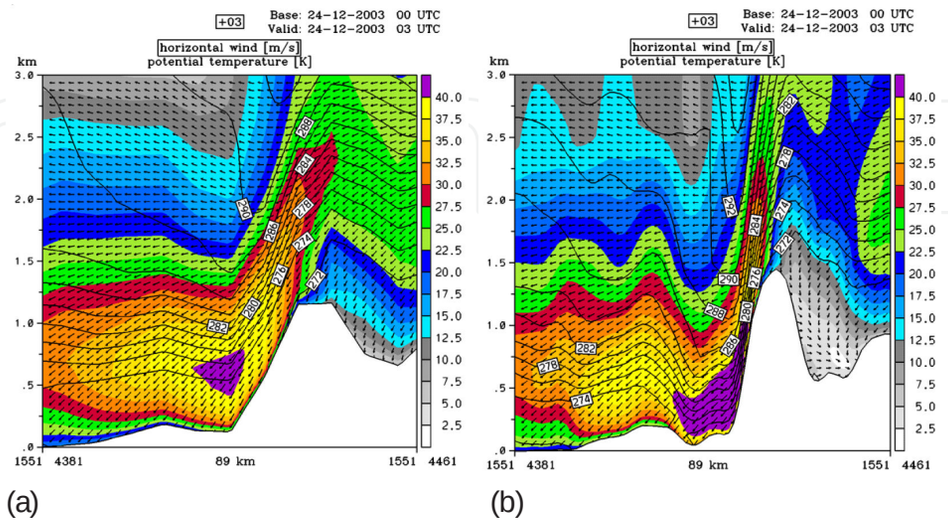

Figure 11. Vertical cross-section of wind speed (shaded), direction (vectors) and potential temperature (black isolines) from 8 km (a) and 2km (b) runs, for 3 UTC 24th Dec 2003.

There were several severe wind episodes in December 2003 (Fig 12), particularly in the period from December 22 to 26 2003, during which infrastructure was damaged on the highway going through the area hit by the severe bura, including the Baričević meteorological station (Fig 12a). The 2 km resolution forecast is in better agreement to the measured data for strong bura events (Fig 12a) as well as the most severe one (Fig 12b). In the absence of atmospheric soundings, these results confirm that the vertical structure of the meteorological fields in the lower troposphere also improves in high resolution for this case.

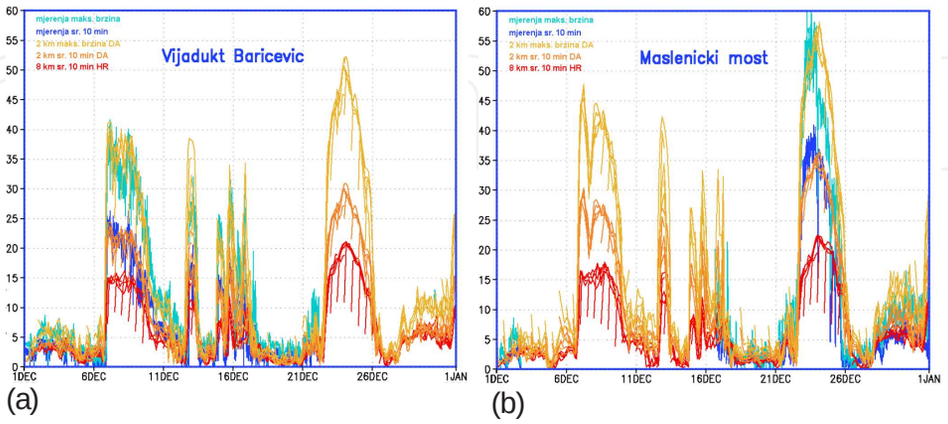

Figure 12. Comparison of measured 10 minute maximum (light blue) and average (blue), 8 km resolution mean wind forecast (red), 2 km resolution mean wind (orange) and wind gust forecast (yellow) at Baričević (a) and Maslenica (b) for December 2003.

http://dx.doi.org/10.5772/55698

3.2. Forecast of the road conditions

The bura variability in space and time has a pronounced influence on road traffic. Therefore, knowing bura characteristics is a necessary condition for road transport safety. To properly organize the traffic safety system, special emphasis should be given to the quality of measured long term wind speed and direction data and low resolution atmospheric forecast models.

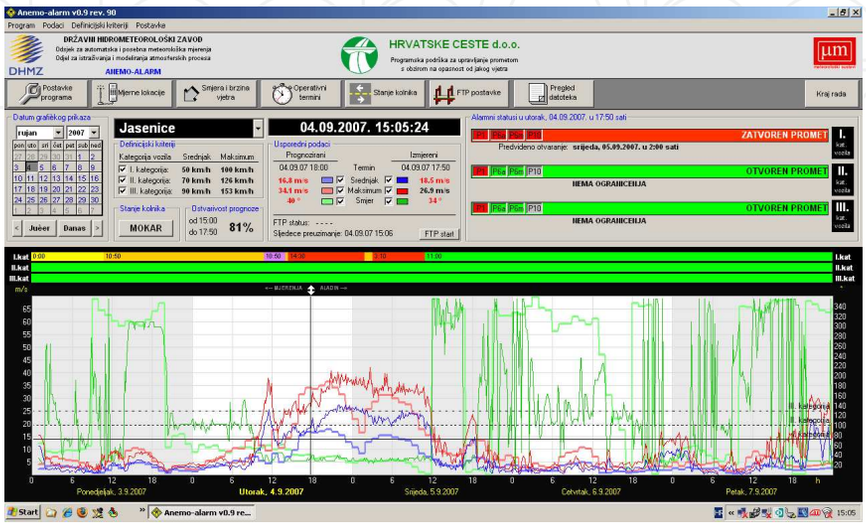

Figure 13. The ANEMO-ALARM user interface. The measured (thick lines) and modelled (thin line) mean wind speed is shown on a graph as blue line, wind gusts are red and direction is green.

An application, named ANEMO-ALARM (Bajić et. al., 2008), has been developed that assists road authorities in managing the traffic on the roads affected by strong wind and turbulence. The application is based on measured and forecasted wind speed and gusts for a choice of locations on Croatian roads that are most affected by severe wind. The application communicates with the user through a graphical user interface (Fig 13). The interface shows current and expected alarm status for road traffic safety conditions for any of the three categories of vehicles (green is for open road, yellow for preparedness status and expected road closure and red indicated that the road is closed).

3.3. Air crash investigation

Prognosed cloud water and ice, rain and snow mixing ratios are valuable output of the operational model forecast. Their three-dimensional distribution helps in identifying the areas that are a potential threat to aviation. This data can provide important information on the state of the atmosphere inside a cloud, especially when in-situ and remote measurements are sparse or insufficient to describe more detailed structure of the cloud. This value is briefly illustrated by means of a case when weather contributed to the crash of an airplane on the Velebit Mountain.

On 5th February 2009, a Cesna 303, crashed 500m north of the Vagan peak of the Velebit Mountain. The small airplane flew from Zagreb to Zadar, first at 2600 m, then at 2000 m feet.

Before the crash, the airplane descended from 1900 to 1600 m. The time of the accident was recorded as 13:53 UTC when air traffic control lost contact with the pilot.

Strong southwest wind prevailed throughout the troposphere. Wind speed increased with height, upstream of the mountain, in Zadar, the maximum wind speed of 20 knots was reached at 750m reaching 45 knots just below 3 km in the Zagreb radiosonde measurements. Temperatures on Zadar airport (88 m) and in Zagreb (128 m) were 14 to 15 °C. On Zavižan peak (1594 m) of the Velebit mountain temperature was 0.3°C, relative humidity was 100% and there was very low visibility, indicating that the mountain top was in a cloud. The satellite images show Velebit mountain covered by a thick cloud and mountain waves in the lee (Fig 14a). The cloud-top temperature was below 0°C (Fig 14b).

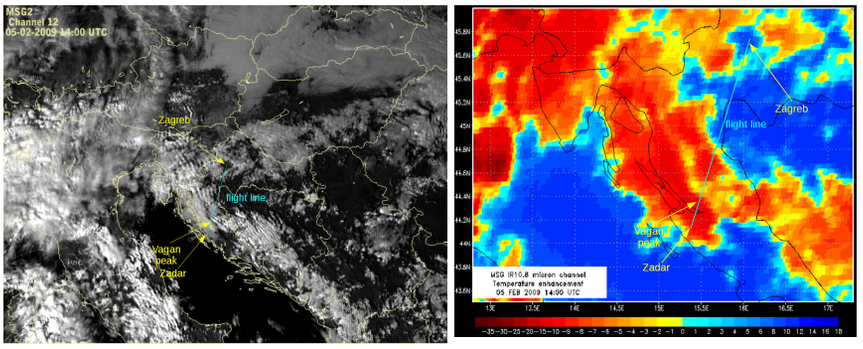

(a) (b)

Figure 14. Satellite picture of clouds (a) and cloud top temperature (b) for 14 UTC 5th Feb 2009.

The model vertical cross-section of vertical velocity and potential temperature (Fig 15a) shows strong downward motion above and north of Vagan peak and variable vertical velocity downstream. Changes in the vertical velocity are accompanied by waves in the isolines of potential temperature (blue lines in Fig 15a). As the airplane flew from Zagreb to Zadar, it faced strong opposing wind and changing upward and downward motions that were stronger as the airplane approached the Vagan peak.

The mountain was covered by layers of clouds consisting of both cloud water and ice (Fig 15b) and high relative humidity existed in the cloud free area. The 0°C-isoline was above the 6500 feet flight level over the valley close to Zagreb, but the 0°C isoline descends below that height above the mountains close to Vagan peak (Fig 15b). Turbulent kinetic energy had high values above and downstream of the mountain (more than $2.5*10^4$ m^2/s^2).

3.4. Jugo (sirocco)

The Adriatic region is often affected by another severe wind that is rather familiar to the local population. Jugo is a local word describing the southeasterly wind in the eastern Adriatic. It interupts the ferry lines to the islands as well as other activities on the sea and the coast since it generates large sea waves due to the long fetch. It is often associated with heavy rainfall. The strength of jugo wind is often underestimated in southern Adriatic, especially in Dubrovnik

http://dx.doi.org/10.5772/55698

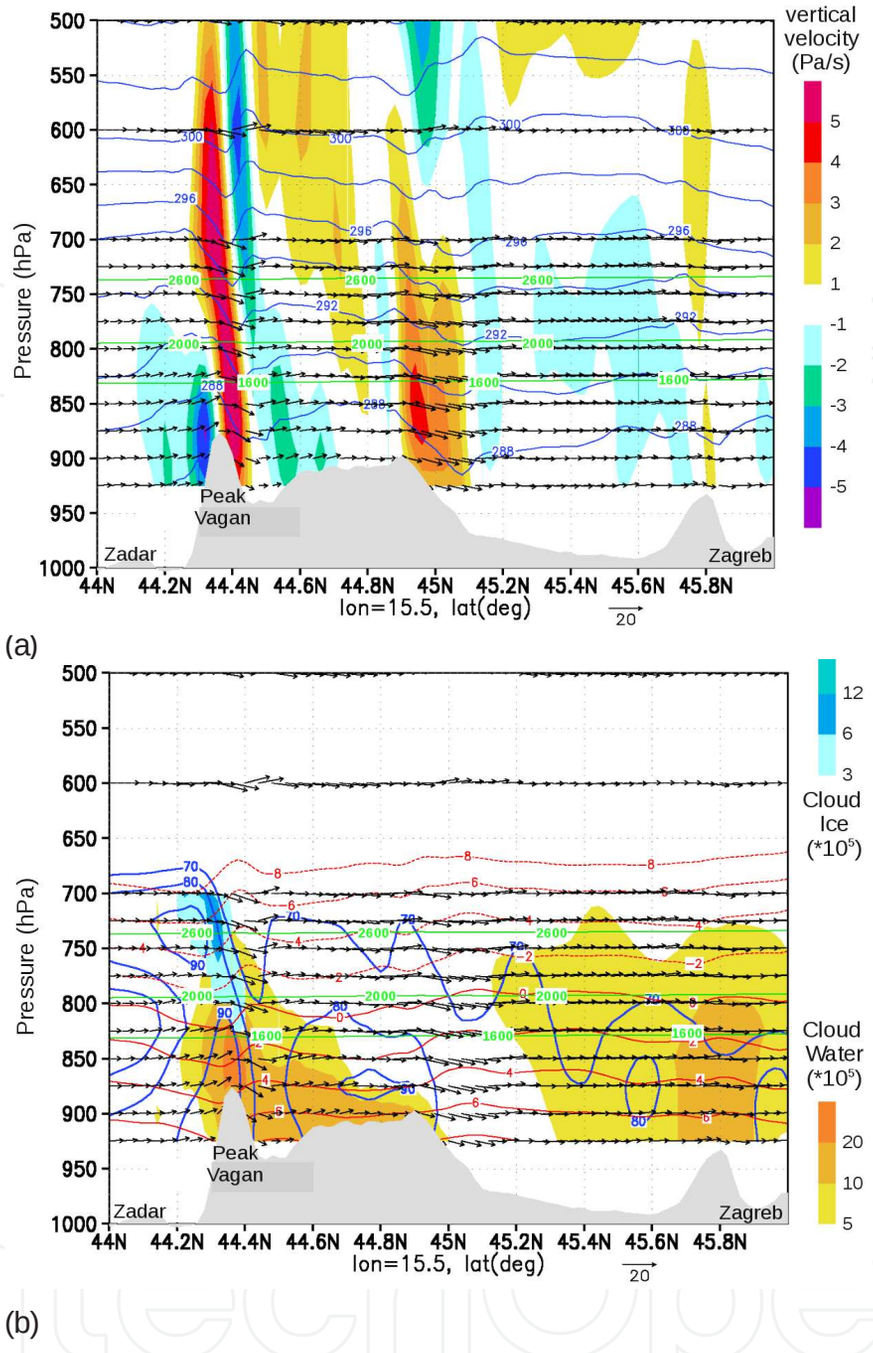

Figure 15. Vertical cross-sections of (a) vertical velocity (shaded), wind vectors parallel to the cross-section (vectors), potential temperature (K, blue lines) and (b) cloud water and ice (shaded), relative humidity (blue lines) and temperature (°C, red lines) for 14 UTC February 5, 2009. The flight levels are shown as horizontal green lines.

and on Palagruža, Lastovo and Vis islands by 15% (2 km resolution) to 30% (8km resolution) on average. The time-variability of jugo wind speed and direction is underestimated over the open sea (at least in some cases), as was revealed in the comparison with the measurements in the open sea during the DART (Dynamics of the Adriatic in Real-Time) oceanic research cruise in March 2006 (Tudor, 2011). The model error of the wind speed forecast is not uniform and can exceed 50% in some intervals for both 8 and 2 km resolution forecast.

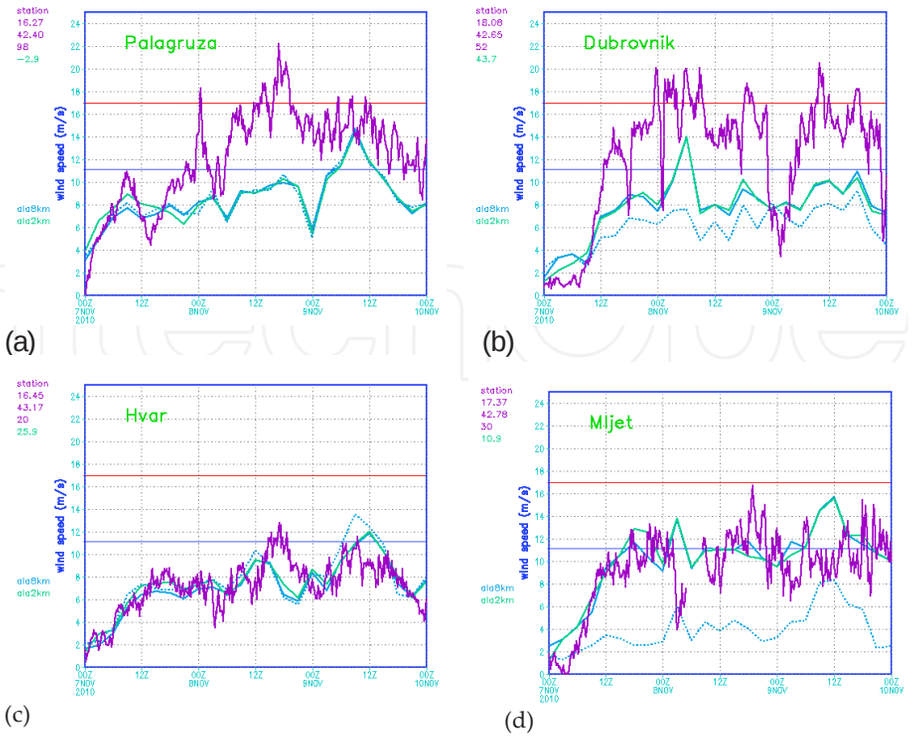

Figure 16. Comparison of measured (purple), 2 km (full lines) and 8 km resolution wind speed forecast (dashed) for Palagruža (a), Dubrovnik (b), Hvar (c) and Mljet (d) for 7th-9th Nov 2010.

3.5. Heavy rain

Large amounts of rain (> 100 mm) that fall during a short time period (< 6 hours) can cause flash floods, especially in places where the terrain supports accumulation of water as on low slope coast below a mountain. The ability of the operational ALADIN model to predict such cases is exemplarily illustrated by two cases.

On September 25, 2010, just after midnight an intensive rain hit Pula city on the southern part of the Istria Peninsula, Croatia. The rain was intensive for several hours and the rainfall rate measured by the ombrograph reached 43.9 mm per hour. Several rain-gauges in the area measured more than 150 mm/24h. The operational ALADIN forecast severely underestimated (the forecast maximum was below 10mm) the rainfall over the Istria peninsula during the night from September 24 to 25, 2010 (Fig 17a). The wind field is shown for 00 UTC on September 25, 2010 the time that is close to the period of the maximum rain intensity. The parallel suite rainfall structures were slightly better (Fig 17b) than the operational one, with second maximum of rainfall over the Istria peninsula reaching more than 35mm, but the predicted rainfall amount was far below the measured one. It is assumed that the observed severe precipitation was caused by convective activity supported by the synoptic conditions and/or local conditions that were not represented correctly in the initial conditions (as suggested by the result of the data assimilation forecast, Fig 17b) or the model was not able to represent its development. The last hypothesis has been tested using the non-hydrostatic set-ups of the ALADIN model and in higher resolution using different initial and boundary conditions (from 8 km runs with

http://dx.doi.org/10.5772/55698

or without 3Dvar and using ARPEGE and IFS initial and boundary conditions) One run generated additional intensive rain band over an island 25 km east of Pula.

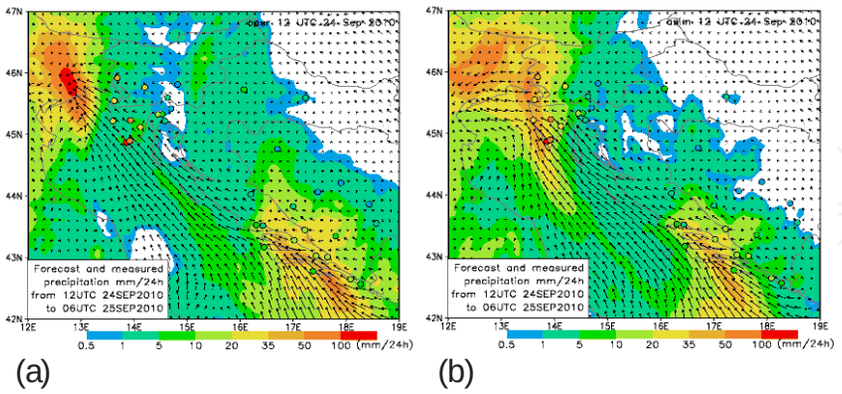

Figure 17. Accumulated precipitation from the operational (a) and data assimilation (b) forecast for 25th Sep 2010.

The flash flood hit Dubrovnik, Croatia, on November 22, 2010. The rain gauge measurements exceeded 100 mm/24h in the area and the one in Dubrovnik measured 161.4 mm/24h (the highest on record by that time), with a peak intensity of 71.5 mm/h (Fig 18b). The flood water level reached 1.5 m caused damage and endangered lives.

The operational and parallel suite model results forecast large 24 hour accumulated rainfall amounts in the area around Dubrovnik, with the maxima over 100 mm located above the surrounding areas of Montenegro and Bosnia and Herzegovina. The results of the high-resolution (2 km) non-hydrostatic ALADIN model run showed a dependency of the forecasts on the input data from initial and lateral boundary conditions. The position and time of the precipitation maxima in the high resolution ALADIN output fields (Fig 18a) was similar to the lower resolution (8 km) run used for initial and lateral boundary conditions. The peak intensity of precipitation in all model runs was late (3 hours in runs coupled to Arpege, 6 hours for IFS). The reason for this delay is yet unknown and could be attributed to the absence of measurements over the southern Adriatic.

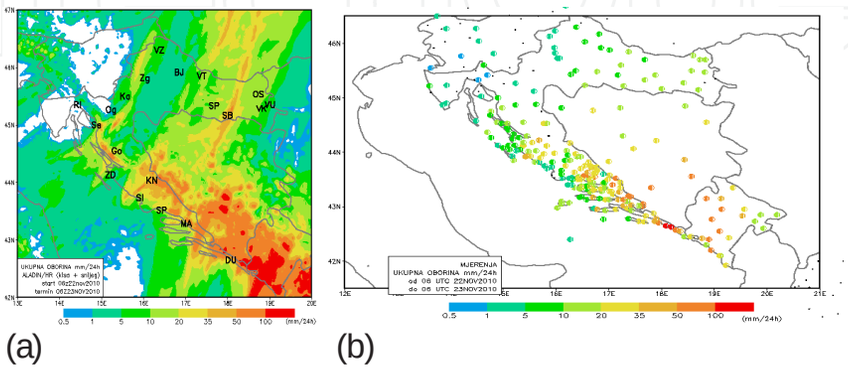

Figure 18. Accumulated 24 h precipitation from the 2 km resolution run (a) and measured (b) for 23rd Nov 2010.

3.6. Fog

Although far less dramatic than the previous ones, fog is also a weather event that can have a large impact since it is a nuisance to the traffic. The results of the operational model forecasts were not satisfactory for 2m temperature and cloudiness in a case of fog and low stratus accompanied with a temperature inversion in December 2004. The problems remained through several weeks of December 2004, as fog and low stratus remained covering the inland parts of Croatia, as well as Hungary and other valleys surrounding eastern Alps.

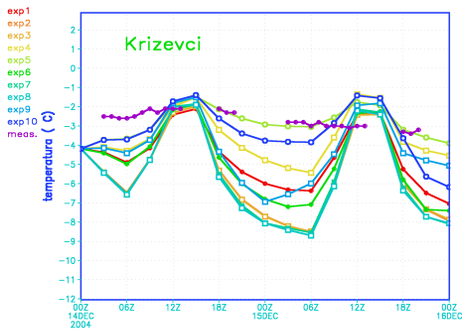

Figure 19. Comparison of the model 2m temperature evolution with the data measured (violet) in Križevci meteorological station. Exp1 to exp5 are obtained with the operational radiation scheme, and in exp6 to exp10 a new, enhanced, radiation scheme has been used. Experiments with random maximum overlap are shown with circles and those with random overlap are shown with squares. Open marks show experiments with the operational critical relative humidity profile and full marks show the experiments with the new critical relative humidity profile.

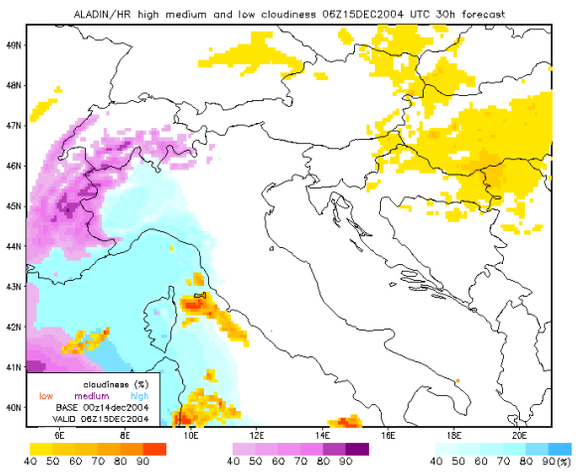

Figure 20. The operational forecast of low (shades of red), medium (shades of violet) and high (shades of blue) cloudiness for 06 UTC on December 15, 2004.

Subsequent operational model forecasts kept underestimating the cloud coverage with 30-60% on average when compared to observations by the crew from the synoptic stations. Consequently, the amplitude of the 2 m temperature diurnal cycle was much larger (5-10°C) than

http://dx.doi.org/10.5772/55698

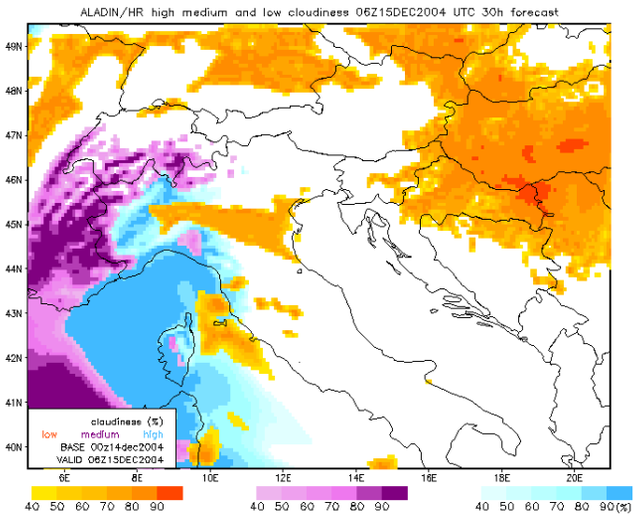

Figure 21. As Fig 20, but obtained from a simulation using the Xu-Randall cloudiness (Xu & Randall, 1996) scheme.

measured (Fig 19). Actually, the measured 2m temperature changed only slightly during the day (0-2°C), as well as from one day to another. This behaviour has made the 2m temperature forecast as useless as the cloudiness forecast.

These results have encouraged an extensive case study to find a model set-up that would produce an acceptable forecast of the low clouds as well as 2m temperature diurnal cycle (Tudor, 2010). The model initially recognizes the existence of the temperature inversion and the layer of air adjacent to the surface is almost saturated. But the cloud scheme diagnoses little cloudiness or fog, far less than exists in reality (Fig 20). Consequently, the radiation scheme heats the ground and breaks the inversion, making the situation even worse. In reality, a fog or low stratus layer keeps the longwave radiation from ground and reflects the shortwave radiation keeping the temperature of the surface layer almost constant. Longwave radiation flux divergence and shortwave reflection at the top of the cloud supports cooling and formation of a temperature inversion.

The study (Tudor 2010) has shown that the combination of Xu-Randall cloud diagnosing scheme (Xu & Randall, 1996), new critical relative humidity profile, maximum overlap and operational (Ritter and Geleyn, 1982) radiation scheme produces forecast of low clouds and 2 m temperature of 1-3°C that is closest to the observed values. This result stayed nearly the same even when the more sophisticated radiation schemes were used. The introduction of prognostic microphysics improved the results too by increasing cloud coverage by 5-10% and reducing the temperature amplitude only slightly (up to 0.3°C). The introduction of more physical semi-Lagrangian horizontal diffusion (SLHD) has improved the fog and low stratus forecast close to terrain slopes by increasing cloud coverage by up to 50%. The numerical diffusion mixes the temperature and moisture along model levels that follow orography. Consequently, in the model the cloud layer from the valley is mixed with the clear air on the mountain ridge and the cloud in the valley reduces. Replacement of numerical diffusion with SLHD reduces this mixing and supports cloud formation on slopes of the valleys.

4. Conclusion

This chapter gives an overview on weather forecasting using the set-up of the NWP model ALADIN that is used for operational weather forecast in CMHS as an example for operation weather forecasting. ALADIN is a state-of-the-art modern NWP model. Using ALADIN we exemplarily discuss short-comings and challenges in modern operational weather forecasting. A high-resolution LAM is intended to predict the sub-synoptic weather features forced by topography or other local characteristics that can be absent in the main synoptic pattern. Successful prediction of these small-scale features enables usage of the LAM forecast in predicting the conditions important for the flight safety, vehicle road safety or navigation at sea. The operational suite has to be tuned in order to predict the high-impact weather events of local character that could be missing in the large scale forecast. The domain properties as well as the forecast model complexity are formed according to the needs of the forecast users and the computing capabilities.

High impact weather events can be of local origin, or determined by small scale characteristics particular to a certain region. Croatia is not spared from severe weather events, such as severe windstorms (bura and jugo wind), torrential rain and flash floods. Such events are often forecast in terms of probability via the ensemble prediction system of a global model. The severity of the event can be controlled by mechanisms not resolved by the global model, and dynamical adaptation of the individual EPS members improves the predictability of the severe weather events (Branković et al., 2007). The NWP section of CMHS has invested most effort in the deterministic high-resolution forecast based on analysis of numerous high impact weather cases.

The operational 8 km resolution forecast is run using DFI with the initial file from the global model ARPEGE since most of the measured data is assimilated in the global model. The data-assimilation suite has been established and runs parallel to the operational suite forecast. This parallel run has revealed the benefits of doing the data-assimilation in higher resolution (8 km) than in the global model (see the Pula flash flood case).

Forecasting the formation and distribution of fog is controlled by subtle variations in humidity and temperature fields and require maintenance of a sensitive balance between the advection, radiation and turbulent fluxes. The profound influence of topography on the atmospheric flow reflects itself in a number of features that affect local weather, such as upslope, downslope and gap winds, coastal barrier jets as well as land sea breezes.

The operational high-resolution (2 km) forecast of the 10 m wind is achieved through the dynamical adaptation method adapted from Žagar & Rakovec (1999). The prediction of severe wind variability and strength is improved in weather situations with strong flow over complex topography, like bura in Croatia (Ivatek-Šahdan & Tudor, 2004). This high resolution wind forecast has provided warnings in numerous cases severe wind as well as to forecast the road conditions, assess the wind energy potential (Horvath et al., 2011) and has been used in numerous applications.

The forecast abilities of HRDA and similar packages are limited to the severe windstorms related to a synoptic forcing. Omitting moist and radiation processes prevents it from being

http://dx.doi.org/10.5772/55698

useful in forecasting other phenomena could benefit from the high resolution, such as local convective storms. The windstorm that is a consequence of a local pressure disturbance requires a full forecast run in 2 km resolution using more complex NH ALADIN model set-up (Tudor & Ivatek-Šahdan, 2010). Several air crash investigations have revealed that this "full-run" high resolution ALADIN forecast enables the prediction of lee waves and zones of increased turbulence as well as icing zones.

These flaws of the operational suite have encouraged the introduction of the 2 km resolution 24 hour forecast with NH ALADIN set-up using the complete set of physics parameterizations to the operational suite at the beginning of summer 2011. Several case studies of high-impact weather phenomena have been used to set-up the model configuration used operationally. The results from these studies have provided encouraging results.

Author details

Martina Tudor, Stjepan Ivatek-Šahdan, Antiono Stanešić, Kristian Horvath and Alica Bajić

Croatian Meteorological and Hydrological Service, Croatia

References

[1] ALADIN International Team, (1997) The ALADIN project: Mesoscale modelling seen as a basic tool for weather forecasting and atmospheric research. *WMO Bull*., 46, 317–324.

[2] Bajić, A. (2003) Očekivani režim strujanja vjetra na autocesti Sv. Rok (jug) – Maslenica. *Građevinar*, 55, 149-158.

[3] Bajić, A., Ivatek-Šahdan, S. & Horvath, K. (2007) Spatial distribution of wind speed in Croatia obtained using the ALADIN model. *Cro. Met. J.* 42 , 67–77.

[4] Bajić, A., Ivatek-Šahdan, S., Žibrat, Z. (2008) ANEMO-ALARM iskustva operativne primjene prognoze smjera i brzine vjetra. *GIU Hrvatski cestar.* 109-114

[5] Berre L. (2000) Estimation of Synoptic and Mesoscale Forecast Error Covariances in a Limited-Area Model, *Mon. Wea. Rev.* 128, 644-667.

[6] Bölöni, G., Horvath K. (2010) Diagnosis and tuning of the background error statistics in a variational data assimilation system. *Időjárás* 114, 1-19.

[7] Branković, Č., Matjačić, B., Ivatek-Šahdan, S. & Buizza, R. (2007) Dynamical down-scaling of ECMWF EPS forecasts applied to cases of severe weather in Croatia. *ECMWF RD Technical Memorandum* 507, 38 pp.

[8] Branković, Č., Matjačić, B., Ivatek-Šahdan, S. & Buizza, R. (2008) Downscaling of ECMWF Ensemble Forecasts for Cases of Severe Weather: Ensemble Statistics and Cluster Analysis. *Mon.Wea. Rev.* 136, 3323–3342.

[9] Brozkova R, Klarić, D., Ivatek-Šahdan, S., Geleyn, J.F., Casse, V., Siroka, M., Radnoti, G., Janousek, M., Stadlbacher, K., Seidl, H. (2001) DFI blending: an alternative tool for preparation of the initial conditions for LAM. WGNE *Blue Book.* 31, 1.7-1.8.

[10] Catry B., Geleyn J.-F., Tudor M., Bénard P. & Trojakova A. (2007). Flux conservative thermodynamic equations in a mass-weighted framework. *Tellus* 59A, pp 71–79

[11] Courtier, 1999: Data assimilation concepts and methods, *ECMWF lecture notes, European Centre for Medium-Range Weather Forecasts*, Reading, England, 59 pp.

[12] Davies, H. C. (1976) A lateral boundary formulation for multilevel prediction models. *Quart. J. Roy. Meteor. Soc.*, 102, 405–418.

[13] Davies, H. (1983) Limitations of some common lateral boundary schemes used in regional NWP models. *Mon. Wea. Rev.*, 111, 1002–1012.

[14] Durran, D.R. (1999) Numerical methods for wave equations in geophysical fluid dynamics. *Springer*, pp 465.

[15] Geleyn J.-F. (1988). Interpolation of wind, temperature and humidity values from model levels to the height of measurement. *Tellus*, 40A, pp.347–351

[16] Geleyn, J.-F., Bazile, E., Bougeault, P., Déqué, M., Ivanovici, V., Joly, A., Labbé, L., Piedélièvre, J.-P., Piriou, J.-M., Royer, J.-F. (1994) Atmospheric parametrizations schemes in Meteo-France's ARPEGE NWP model. *ECMWF seminar proceedings on Parametrization of sub-grid scale physical processes,* pp. 385-402.

[17] Geleyn J.-F. & Hollingsworth A (1979) An economical analytical method for the computation of the interaction between scattering and line absorption of radiation. *Beitr Phys Atmos* 52:1–16.

[18] Geleyn J.-F., Benard P. & Fournier, R. (2005a) A general-purpose extension of the Malkmus band-model average equivalent width to the case of the Voigt line profile. *Quart. J. Roy. Meteor. Soc.* 131:2757–2768

[19] Geleyn J.-F., Fournier R., Hello G., Pristov N. (2005b) A new 'bracketing' technique for a flexible and economical computation of thermal radiative fluxes, scattering effects included, on the basis the Net Exchanged Rate (NER) formalism. WGNE Blue Book

[20] Geleyn J.-F., Vana F., Cedilnik J., Tudor M. & Catry B. (2006). An intermediate solution between diagnostic exchange coefficients and prognostic TKE methods for vertical turbulent transport. *WGNE Blue Book*

[21] Geleyn J.-F., Catry B., Bouteloup Y. & Brožkova, R. (2008). A statistical aproach for sedimentation inside a microphysical precipitation scheme. *Tellus* 60A,649–662

[22] Gerard, L. (2007) An integrated package for subgrid convection, clouds and precipitation compatible with the meso-gamma scales. *Quart. J. Roy. Meteor. Soc*., 133, 711–730.

[23] Gerard, L. & Geleyn, J.-F. (2005) Evolution of a subgrid deep convection parametrization in a limited area model with increasing resolution. *Quart. J. Roy. Meteor. Soc.*, 131, 2293–2312.

[24] Gerard, L., Piriou, J.-M., Brožková, R., Geleyn, J.-F. & Banciu, D. (2009) Cloud and Precipitation Parameterization in a Meso-Gamma-Scale Operational Weather Prediction Model. *Mon. Wea. Rev.*, 137, 3960–3977.

[25] Giard, D. and Bazile, E. (2000) Implementation of a new assimilation scheme for soil and surface variables in a global NWP model. *Mon. Wea. Rev.* 128, 997-1015.

[26] Gospodinov, I., Spiridonov, V., & Geleyn, J.-F., (2001) Second order accuracy of two-time-level semi-Lagrangian schemes. *Quart. J. Roy. Meteor. Soc.*, 127, 1017–1033.

[27] Grisogono, B., Belušić, D. (2009) A review of recent advances in understanding the meso- and microscale properties of the severe Bora wind. *Tellus* 61A, 1–16.

[28] Grubišić, V. (2004) Bora-driven potential vorticity banners over the Adriatic. *Quart. J. Roy. Meteor. Soc. 130*, 2571-2603.

[29] Haugen, J. E. & Machenhauer, B. (1993) A spectral limited-area model formulation with time-dependent boundary conditions applied to the shallow-water equations. *Mon. Wea. Rev.*, 121, 2618–2630.

[30] Hdidou, F.Z., (2006) Test of an assimilation suite for ALBACHIR based on the variational technique. available at www.wmo.int

[31] Hólm, E.V., 2008: Lecture notes on assimilation algorithms. *ECMWF, European Centre for Medium-Range Weather Forecasts*, Reading, England, 30 pp.

[32] Hollingsworth, F. Rabier and M. Fisher, 1998: The ECMWF implementation of three-dimensional variational assimilation (3d-Var). I: Formulation. *Quart. J. Roy. Meteor. Soc.*, 124, 1783-1807.

[33] Horvath, K., Bajić, A., & Ivatek-Šahdan, S. (2011) Dynamical Downscaling of Wind Speed in Complex Terrain Prone To Bora-Type Flows. *J. Appl. Meteor. Climatol*., 50, 1676–1691.

[34] Horvath, K., Ivatek-Šahdan, S., Ivančan-Picek, B. & Grubišić, V. (2009) Evolution and structure of two severe cyclonic bora events: contrast between the northern and southern Adriatic. *Weather and forecasting* 24, 946-964.

[35] Ivatek-Šahdan, S. & Ivančan-Picek, B. (2006) Effects of different initial and boundary conditions in ALADIN/HR simulations during MAP IOPs. Meteorol. Z. 15, 187–197.

[36] Ivatek-Šahdan, S. & Tudor M. (2004) Use of high-resolution dynamical adaptation in operational suite and research impact studies. *Meteorol Z* 13(2):1–10

[37] Kann A., Seidl H., Wittmann C. & Haiden T. (2009) Advances in predicting continental low stratus with a regional NWP model. *Wea. Forecasting*, 25, 290–302.

[38] Kessler E. (1969) On distribution and continuity of water substance in atmospheric circulations. *Meteorol Monogr Am Meteorol Soc* 10(32):84

[39] Louis J.-F., Tiedke M. & Geleyn J.-F. (1982) A short history of PBL parameterization at ECMWF. In: *Proceedings from ECMWF workshop on planetary boundary layer parameterization, 25–27 November 1981*, pp 59–79

[40] Lynch, P., X.-Y. Huang (1994) Diabatic Initialization using recursive filters. – *Tellus* 46A, 583–597.

[41] Machenhauer, B., J.E. Haugen (1987) Test of a spectral limited area shallow water model with timedependent lateral boundary conditions and combined normal mode/ semi-lagrangian time integration schemes. *Techniques for Horizontal Discretization in Numerical Weather Prediction Models, 2–4 November 1987*, ECMWF, 361–377.

[42] Mahfouf, J.,F., 1991: Analysis of soil moisture from near-surface variables: A feasibility study. *J. Appl. Meteor.*, 30, 1534-1547

[43] Mlawer E.J., Taubman S.J., Brown P.D., Iacono M.J. & Clough S.A. (1997) Radiative transfer for inhomogeneous atmospheres: RRTM, a validated correlated-k model for the longwave. *J Geophys Res* 102D:16663–16682

[44] Morcrette J.-J. (1989) Description of the radiation scheme in the ECMWF Model. *Tech Memo 165, ECMWF*, 26 pp

[45] Noilhan, J., Planton, S. (1989) A simple parapetrization of land surface processes for meteorological models. *Mon. Wea. Rev.* 117, 536-549.

[46] Pauluis O., Emanuel K. (2004) Numerical instability resulting from infrequent calculation of radiative heating. Mon Weather Rev 132:673–686

[47] Pielke, R.A. (2002) Mesoscale meteorological modelling. *Academic press*, pp 676.

[48] Radnóti, G. (1995) Comments on ''A spectral limited-area formulation with time-dependent boundary conditions applied to the shallow-water equations". *Mon. Wea. Rev.*, 123, 3122– 3123.

[49] Redelsperger J.L., Mahé F., Carlotti P. (2001). A simple and general subgrid model suitable both for surface layer and free-stream turbulence. *Bound.-Layer Meteor.* 101, pp.375–408.

[50] Ritter B. & Geleyn J.-F. (1992) A comprehensive radiation scheme for numerical weather prediction models with potential applications in climate simulations. *Mon Wea. Rev* 120:303–325

[51] Robert, A. (1982) A semi-Lagrangian and semi-implicit numerical integration scheme for the primitive equations. *J. Meteor. Soc. Japan*, 60, 319-325.

[52] Simmons, A.J., Burridge, D.M. 1981: An Energy and Angular-Momentum Conserving Vertical Finite-Difference Scheme and Hybrid Vertical Coordinates. *Mon. Wea. Rev.* 109, 758–766.

[53] Staniforth A, Côté J. (1991) Semi-Lagrangian integration schemes for atmospheric models – A review. *Mon. Wea. Rev*. 119 2206–2223.

[54] Termonia, P. (2008) Scale-selective digital filtering initialization. *Mon. Wea. Rev.*, 136, 5246–5255.

[55] Tudor M. (2010). Impact of horizontal diffusion, radiation and cloudiness parameterization schemes on fog forecasting in valleys. *Met. Atm. Phy.* Vol.108, pp. 57-70.

[56] Tudor, M. (2011). The meteorological aspects of the DART field experiment and preliminary results. *Cro. Met. J.* 44/45, 31-46.

[57] Tudor, M. & Ivatek-Šahdan, S. (2002) The MAP-IOP 15 case study. *Cro. Met. J*. 37, 1-14.

[58] Tudor, M. & Ivatek-Šahdan, S. (2010) The case study of bura of 1st and 3rd February 2007, *Meteorol. Z.*, 19, pp. 453-466.

[59] Tudor, M., Termonia, P., (2010) Alternative formulations for incorporating lateral boundary data into limited-area models. *Mon. Wea. Rev.* 138, pp. 2867-2882.

[60] Unden, P., Rontu, L., Jarvinen, H., Lynch, P., Calvo, J., Cats, G., Cuxart, J., Eerola, K., Fortelius, C., Garcia-Moya, J.A., Jones, C., Lenderlink, G., McDonald, A., McGrath, R., Navascues, B., Nielsen, N., Odegaard, V., Rodriguez, E., Rummukainen, M., Room, R., Sattler, K., Hansen Sass, B., Savijarvi, H., Schreur, B., Sigg, R., The, H., Tijm, S., (2002) HIRLAM-5 scientific documentation. *SMHI, S-601 76 Norrkoping, Sweden*, pp 146, available at www.hirlam.org

[61] Váňa F., Bénard P., Geleyn J.-F., Simon A. & Seity Y. (2008). Semi-Lagrangian advection scheme with controlled damping–an alternative way to nonlinear horizontal diffusion in a numerical weather prediction model. *Quart. J. Roy. Meteor. Soc*, Vol.134, pp. 523–537.

[62] Wang, Y., Bellus, M., Wittmann, C., Steinheimer, M., Weidle, F., Kann, A., Ivatek-Šahdan, S., Tian, W., Ma, X., Tascu, S., Bazile, E. (2011) The Central European limited-area ensemble forecasting system: ALADIN-LAEF. *Quart. J. Roy. Meteor. Soc* 137, 483-502.

[63] Warner, T., Peterson, R., Treadon, R. (1997) Atutorial on lateral boundary conditions as a basic and potentially serious limitation to regional numerical weather prediction. *Bull. Amer. Meteor. Soc*., 78, 2599–2617.

[64] Xu K.-M. & Randall D.A. (1996) A semi-empirical cloudiness parameterization for use in climate models. *J Atmos Sci* 53:3084–3102

[65] Yessad, K (2011) Library architecture and history of the technical aspects in ARPEGE/IFS, ALADIN and AROME in the cycle 37 of ARPEGE/IFS. *Meteo-France,* pp. 22, available at http://www.cnrm.meteo.fr/gmapdoc/IMG/pdf/ykarchi37t1.pdf

[66] Zaninović, K., Gajić-Čapka, M., Perčec Tadić, M., Vučetić, M., Milković, J., Bajić, A., Cindrić, K., Cvitan, L., Katušin, Z., Kaučić, D., Likso, T., Lončar, E., Lončar, Ž., Mihajlović, D., Pandžić, K., Patarčić, M., Srnec, L., Vučetić, V., (2008) Climate atlas of Croatia: 1961. - 1990. : 1971. - 2000. . Zagreb : CMHS *Monograph,* pp. 200.

[67] Žagar, M., Rakovec, J. (1999): Small-scale surface wind prediciton using dynamical adaptation. *Tellus,* Vol.51A, pp. 489–504.